DnaJ, A Promising Vaccine Candidate Against *Ureaplasma Urealyticum* Infection

Fangyi Guo
University of South China
Yanhong Tang
Guangzhou Medical University
Wenjun Zhang
University of South China
Hongxia Yuan
The First People's Hospital of Chenzhou
Jing Xiang
The First People's Hospital of Chenzhou
Wenyou Teng
The First People's Hospital of Chenzhou
Ranhui Li
University of South Chian
Guozhi Dai (daigz008@126.com)
University of South China

Research Article

Keywords: recombinant vaccine, DnaJ, Ureaplasma urealyticum, heat shock proteins, bone marrow-derived dendritic cells

Posted Date: December 6th, 2021

DOI: https://doi.org/10.21203/rs.3.rs-1132437/v1

Abstract

Background: *Ureaplasma urealyticum* (Uu) is an important sexually transmitted pathogen that is responsible for diseases such as non-gonococcal urethritis, chorioamnionitis and neonatal respiratory diseases. The rapid emergence of multidrug-resistant bacteria threatens the effective treatment of *U. urealyticum* infections. Considering this, vaccination could be an efficacious medical intervention to prevent *U. urealyticum* infection and disease. As a highly conserved molecular chaperone, DnaJ is expressed and upregulated by pathogens soon after infection. Here, we assessed the potential of recombinant DnaJ vaccine in a mouse model and dendritic cells (DCs).

Results: The results showed that intramuscular administration of recombinant DnaJ induced robust humoral- and T helper (Th) 1 cell-mediated immune responses and protected against cervical infection, inflammation, and the pathologic sequelae after *U. urealyticum* infection. Importantly, DnaJ also induced the maturation of mouse bone marrow-derived DCs (BMDCs), ultimately promoting naïve T-cell differentiation towards the Th1 phenotype. In addition, adoptive immunisation of DnaJ-pulsed BMDCs elicited antigen-specific immunoglobulin G2 antibodies as well as a Th1-biased cellular response in mice.

Conclusion: We concluded that DnaJ can be a promising vaccine candidate to control *U. urealyticum* infections.

Background

Ureaplasma urealyticum is a sexually transmitted pathogen that is commonly found in the genitourinary tract of both males and females [1]. *U. urealyticum* infection is frequently asymptomatic and chronic with clinical manifestations [2]. However, in some individuals, *U. urealyticum* causes non-gonococcal urethritis, atypical neonatal respiratory diseases, chorioamnionitis, pre-term premature rupture of membranes, intraventricular haemorrhage, hyperammonaemia and cerebral oedema [3–5]. Moreover, this sexually transmitted bacterium is resistant to several antibiotics, including levofloxacin, ciprofloxacin, tetracycline, erythromycin, azithromycin, doxycycline, ofloxacin and josamycin [6–9]. Given the serious sequelae and resistance to broad-spectrum antibiotics, the isolation and characterisation of novel immunological targets against *U. urealyticum* to develop an effective vaccine is urgently required. Immunisation is the most effective and economical approach, as premeditated eradication is better than repeated recurrences [10]. Although numerous vaccination strategies against *U. urealyticum* are being developed, no licensed vaccine is currently available.

Inside host immune cells such as macrophages and dendritic cells (DCs), *U. urealyticum* encounters various stressful conditions. Previously, we found that host oxidative stress could be an important aspect of *U. urealyticum* pathogenesis [11,12]. Therefore, to combat oxidative stress such as heat shock and nutrient deprivation, the invading pathogens usually express a large heat shock protein (HSP) repertoire that helps them survive [13,14]. In recent years, growing evidence has revealed that bacterium-derived HSP70 is essential for DC maturation and lymphocyte activation and is highly immunogenic during

infections [15,16]. In *U. urealyticum*, the HSP70 system comprises GrpE (Uu0450)-DnaK (Uu0346)-DnaJ (Uu0451), and the genes for these three proteins are expressed together [17]. Previously, we found that vaccination with recombinant *U. urealyticum* (Uu)-GrpE led to a decrease in the pathogen burden and inflammatory responses in the cervical tissues in a BALB/c mouse *U. urealyticum* vaginal-challenge model [18]. However, Uu-DnaJ, as a candidate vaccine molecule, has received relatively less attention.

In the present study, we aimed to investigate if vaccination with recombinant DnaJ (with Freund's adjuvant) induces antigen-specific antibodies and cell-mediated immune responses to eliminate *U. urealyticum*. In addition, we aimed to assess the effects of Uu-DnaJ on bone marrow-derived DC (BMDC) activation and their subsequent effect on the T-helper (Th) 1 cell-biased response, which could tentatively indicate that DnaJ immunisation could induce a Th1 immune cascade-related reaction and, consequently, efficiently protect mice against *U. urealyticum* infection.

Methods

DnaJ protein sequence retrieval

The complete (Uniprot Accession No. B5ZBQ4) amino acid sequence of *U. urealyticum* DnaJ was obtained from UniProt (http://www.uni-prot.org) in the FASTA format.DnaJ sequence conservation across different serovars of *U. urealyticum* was analysed using BLASTp, with a sequence identity of >95% and coverage percentage of >95%.

Analysis of physicochemical properties

Three physiochemical properties of the *U. urealyticum* DnaJ protein were analysed, including the theoretical number of transmembrane helices, MW and pI. The MW and pI were determined using Expasy ProtParam (https://web.expasy.org/protparam/). Transmembrane helices were studied using TMHMM (https://services.healthtech.dtu.dk/service.php?TMHMM-2.0), with a cut-off <1.

Structure prediction and assessment

The Phyre2 server (http://www.sbg.bio.ic.ac.uk/phyre2/) was used to predict the DnaJ 3D structure. Validation of the predicted 3D model through the generation of a Ramachandran plot was performed using PdbSum (http://www.ebi.ac.uk/thornton-srv/databases/pdbsum/Generate.html).

Antigenic epitope mapping

To determine the B-cell candidate linear epitopes, the full-length DnaJ protein sequence was analysed using BepiPred 2.0, with a 0.55 cut-off and a 15-me epitope length, and using ABCpred, with a 0.80 threshold value and a 16-me epitope length. Next, ElliPro (http://tools.iedb.org/ellipro/), available in

IEDB, was used to perform structural B-cell epitope prediction, with a threshold value of >0.5, using the 3D model of DnaJ. Finally, the antigenicity of the linear and structural B-cell epitopes was further assessed using Vaxijen V2.0 (http://www.ddg-pharmfac.net/vaxijen/VaxiJen/VaxiJen.html).

To predict CTL epitopes, we followed the method reported by Paul et al. [19], scoring all peptides with the frequent HLA allele models, selecting the top 1% scoring peptides in the DnaJ sequence. For the helper T-lymphocyte epitope prediction, we applied a previously reported method with modifications [20], using the Tepitool resource in IEDB and a median consensus percentile of <20, which corresponds to a target-specificity threshold of 50%.

U. urealyticum and culture conditions

The standard strain of *U. urealyticum* serovar 8 (ATCC 27618) was cultivated in a pleuropneumonia-like organism with 16% foetal bovine serum (FBS, Gibco), 0.3% urea, 0.002% phenol red and 1,000 U/mL penicillin G. As described previously, *U. urealyticum* culture dilutions were inoculated onto a solid medium and incubated at 37 °C for 5 days to determine CFUs.

Recombinant DnaJ (rDnaJ) expression and purification

The genomic DNA (gDNA) of *U. urealyticum* strain 8 was used as a template for PCR to amplify the full-length DnaJ gene sequence. The following primers were used: forward primer, 5'-CG**GGATCC**ATGGCGAAACGTGACTACTACG-3' (the BamHI site is underlined), and reverse primer, 5'-CCG**CTCGAG**TTACTGCATCAAGCGGAGTTATTTGTTCACTTCTTTCAGCAGTTT-3'

(the XhoI site is underlined). The target DnaJ fragment (1,128 bp) was cloned into the expression vector pET28a using the BamHI and XhoI restriction sites, which harbour the His6 tag at the N-terminus. Recombinant pET28a-DnaJ was transformed into *E. coli* BL21 (DE3) cells. Before expression, the target DnaJ fragment integrity in the vector was confirmed by double digestion and sequencing.

rDnaJ expression was induced by 100 μg/mL kanamycin and 0.5 mM IPTG at 37 °C for 4 h. Bacterial cells were harvested and re-suspended in lysis buffer (10 mM imidazole, 20 mM NaH_2PO_4, 50 mM Tris-HCl (pH 7.8), 300 mM NaCl, 20% glycerol and 1% Triton X-100). For easy purification, rDnaJ with a His6 tag was expressed as a soluble protein, purified by Ni-NTA affinity chromatography, and step-eluted with different concentrations of imidazole (100–300 mM). The purified recombinant protein was investigated by 12.5% SDS- PAGE. Once purified, DnaJ was treated with ToxinEraser ™ Endotoxin Removal Kit (GenScript, Piscataway, NJ).

Mice

Studies were performed on 4–6-week-old female BALB/c mice and C57BL/6 mice from the Hunan SJA Laboratory Animal Co., China (Approval No. SCXK-Hunan-2019-0004). Specific-pathogen-free mice were housed in a barrier facility and handled by authorised personnel. All protocols were approved by the Institutional Animal Use Committee of the University of South China.

BMDC generation and stimulation

BMDCs were generated from C57BL/6 bone marrow precursors according to a previously described procedure [21, 22]. Briefly, the bone marrow precursors were differentiated for 6 d in Rosewell Park Memorial Institute (RPMI)-1640 with 15% FBS, 10 ng/mL granulocyte-macrophage colony-stimulating factor (R&D Systems), 10 ng/mL IL-4 (PeproTech) and 100 U/mL penicillin/streptomycin at 37 °C with 5% CO_2. Flow cytometric analysis confirmed that the isolated cell purity was approximately 90% (Supplementary Figure 1). Immature BMDCs (5×10^6 cells/well) were plated onto 24-well plates and pulsed with DnaJ.

Cytotoxic assay

The BMDCs in the 24-well plates were incubated with DnaJ (5–80 μg/mL) for 48 h. The culture supernatant was collected and LDH activity was measured using a microplate reader at 570 nm.

Immunisation protocols

Purified recombinant protein Uu-DnaJ (50 μg), emulsified with 100 μL of Freund's complete adjuvant (Sigma-Aldrich, St. Louis, MO, USA) for the first inoculation (injected intramuscularly, 0 weeks), followed by two booster inoculations at 2-week intervals with Freund's incomplete adjuvant (2 and 4 weeks). Negative control mice were injected with equal amounts of PBS or FA (PBS was emulsified in FA) at the immunising site. Serum samples were collected from the tail vein of each mouse weekly (0, 1, 2, 3, 4, 5 and 6 weeks). Two weeks after the last immunisation, the mice were euthanised and splenocytes were isolated for the immunoassays.

Genital tract infection challenge

Groups of mice were challenged with 1×10^7 CFU *U. urealyticum* (re-suspended in 30 μL of PBS) intravaginally 2 weeks after the last immunisation. Prior to the challenge, the oestrus cycle was synchronised by neck subcutaneous treatment with oestradiol benzoate (0.5 mg/mouse), increasing susceptibility to *U. urealyticum* infection. At weeks 0, 1, 2 and 3 after the genital challenge, vaginal or cervical samples were collected using swabs. Then, *U. urealyticum* was cultured in the samples, as previously described.

Western blot analysis

Three microliters of DnaJ lysate was separated by SDS-PAGE in a 12.5% gel and blotted onto a previously rehydrated polyvinylidene fluoride membrane. After 3 h of blocking with 5% skimmed milk and washing twice with Tris-buffered saline with Tween-20 (TBST), the membrane with the protein was incubated with DnaJ-immunised mouse serum or (Uu-serum) as the primary antibody and then kept overnight at 4 °C on a shaker. The following day, after four washes with TBST, the bands were incubated with anti-mouse IgG antibodies conjugated with horseradish peroxidase (HRP, 1:5,000) (Cell Signaling Technology, MA, USA) for 1.5 h at 37 °C. After the blots were rewashed with TBST, they were exposed to a chemiluminescence instrument (CLINX-6300, China). Finally, images were obtained using a film developer (EPSON-V370, Japan).

ELISA

The antigen-specific antibody responses were assayed using ELISA in 96-well plates. For the antibody titres, the plates were coated with purified rDnaJ (10 µg/mL, 100 µL/well) overnight at 4 °C. The microplates were then blocked with 5% skim milk at 37 °C for 2 h. After blocking, the microplates were washed four times with PBS containing Tween 20 (PBST). The serum samples were serially diluted from 1:100 to 1:204,800 in dilution buffer, and 100 µL of the diluted serum was added to each well. After 2 h of incubation at 37 °C, the microplates were washed six times with PBST and HRP-conjugated goat anti-mouse IgG (1:10,000) was distributed into each well for 1 h at 37 °C. Then, 3,3’,5,5’-tetramethylbenzidine (substrate (100 µL/well) was added, the microplates were incubated at 37 °C for 20 min and the reaction was stopped using 2N H_2SO_4. The absorbance of the plates was measured at 450 nm using a microplate reader (Multiskan Mk-3, Thermo Fisher Scientific). The antibody titres were determined as the highest dilution of serum giving a detectable absorbance reading 2.1 times above the background average.

To further measure the serum IgG, IgA, IgM, IgG1, IgG2a, IgG2b and IgG3 responses, the microplates were coated with DnaJ. On the following day, the plates were incubated with the serum samples from the mice (1: 100 diluted in 5% non-fat milk in PBST). Horseradish peroxidase-conjugated goat anti-mouse IgA, IgM, IgG1, IgG2a, IgG2b or IgG3 was added at a 1:1,000 dilution to the designated well, following the same procedure as above.

Cytokine quantification

Cytokine levels were determined in mouse splenocytes and BMDCs. The splenocytes were cultured at 2 × 10^6 cells/well in 24-well plates and stimulated with DnaJ (10 µg/mL) for 48 h. Alternatively, BMDCs (5 × 10^6 cells/well) were treated with 5–20 µg/mL DnaJ for 24 h. Then, supernatants were collected to measure the levels of secreted cytokines such as IFN-γ, TNF-α, IL-4, IL-10, IL-1β, IL-6 and IL-12p70 using

the corresponding mouse ELISA kits, according to the manufacturer's instructions (eBioscience, San Diego, USA).

Flow cytometry analysis

Mouse BMDCs or splenocytes were washed with BD Pharmingen Stain Buffer. For surface marker extracellular staining, the cells were incubated with anti-mouse CD11c (557400, BD Biosciences), CD80 (560526, BD Biosciences), CD86 (552692, BD Biosciences), MHC-II (562367, BD Biosciences), CD4 (553046, BD Biosciences) or CD8 antibodies (551162, BD Biosciences) at 4 °C for 30 min. For intracellular cytokine staining, the splenocytes were seeded at 37 °C for 8 h in Uu-DnaJ (10 μg/mL) of Golgi plug^{TM} (51-2301KZ, BD Bioscience). The splenocytes were then treated for surface markers (CD4 or CD8), fixed/permeabilised with a Cytofix/Cytoperm solution (BD Bioscience) and then stained with anti-IFN-γ (557735, BD Biosciences) and anti-IL-4 (554435, BD Biosciences) antibodies at 20–25 °C for 30 min. All events were acquired on a FACSverse flow cytometer and analysed using the FlowJoV software (Tree Star).

To determine cytokine (IFN-γ, TNF-α, IL-1β, IL-10, IL-17a, (MCP-1), IL-1α and IL-6) concentrations in the cervical tissue, multi-analyte flow assay kits (Biolegend, San Diego, CA, USA) were used as indicated by the manufacturer.

Quantitative real-time polymerase chain reaction(qPCR)

U. urealyticum loads in the cervical tissue were determined as previously described [18]. In short, 14 days after infection, mice were anesthetised and euthanised and the whole cervix was rapidly harvested and stored at −80 °C. gDNA from the cervix was extracted and qPCR was performed using gene-specific primers (*U. urealyticum* urease gene) on a Light Cycle 96 apparatus (Roche, Basel, Switzerland).

Histopathology

The mice were immunised with DnaJ and challenged with *U. urealyticum*, as described above. The reproductive tract was removed from immunised mice 14 days after infection, fixed with 4% paraformaldehyde and embedded in paraffin, and the paraffin-embedded reproductive tract samples (including the uterine horn) were cut into sections. For routine histology, the cervical tissue sections were stained with haematoxylin and eosin. In addition, to visualise the pathogen load in the mouse cervical tissues, immunohistochemical detection of *U. urealyticum* antigen was performed as described previously [18], and mouse anti-*U. urealyticum* was provided by the Pathogenic Biology Institute (University of South China, Hunan, China). All cervical tissue sections were blindly evaluated by two pathologists.

Detection of endotoxin removal effect in DnaJ

The endotoxin removal effect in the rDnaJ detection method was modified from a previous study[21]. DnaJ was incubated in PBS containing 10 μg/mL PMB for 3 h at 4 °C. Moreover, for heat-inactivation (Boiling), DnaJ was incubated at 100 °C for 2 h. After 24 h of antigen pulsing, the surface molecules (CD80, CD86 and MHC-II) expression levels in $CD11c^+$ BMDCs were measured by flow cytometry analysis.

BMDC and naïve T-cell co-culture

The allogeneicT cells were isolated from BALB/c mouse splenocytes using MojoSort™ Mouse Naïve CD4T cell Isolation Kit (480040, BioLegend) and co-cultured with BMDCs at a ratio of 1:10 for 3 days. The levels of IFN-γ, IL-4, IL-5 and IL-10 were quantified on the culture supernatant using commercially available ELISA kits (eBioscience, San Diego, USA).

Adoptive immunisation with DnaJ-pulsed BMDCs

The BMDCs were cultured and stimulated as described above. Six-week-old female C57BL/6 mice (four per group) were immunised with intravenous injection of 2×10^6 mature DnaJ-pulsed BMDCs. Booster immunisation was performed with the same number of DnaJ-pulsed BMDCs at 7-day intervals. Control groups were injected with equal amounts of PBS or untreated BMDCs. Serum was collected from all mice and these were sacrificed to isolate splenocytes for subsequent experiments (ELISA or flow cytometry analysis).

Statistical analyses

Statistical analysis was performed using one-way ANOVA followed by the Duncan test. All results are expressed as mean ± standard error of the mean. Prism version 8 software (GraphPad Inc, San Diego, CA, USA) was used for analysis. P-values lower than 0.05 were considered significant.

Results

DnaJ is conserved among the U. urealyticum serovars

The BLASTp analysis results indicated that the DnaJ protein sequence revealed a high sequence conservation degree (sequence similarity >99%) among the different *U. urealyticum* serovars, thus acting as an effective target for broad-spectrum vaccine development (Table 1).

Table 1. Evaluation of the conservative distribution of Uu-DnaJ protein sequences.

Order	Serovars	Identities (%)	Positives (%)	Gaps (%)	E Value
1	Serovar 2	100%	100%	0	0
2	Serovar 4	100%	100%	0	0
3	Serovar 5	100%	100%	0	0
4	Serovar 7	100%	100%	0	0
5	Serovar 8	100%	100%	0	0
6	Serovar 9	99%	99%	0	0
7	Serovar12	100%	100%	0	0
8	Serovar 13	100%	100%	0	0

Physicochemical property assessment

The *U. urealyticum* DnaJ protein contains 375 amino acids with a molecular weight (MW) of approximately 41.79 kDa and a theoretical isoelectric point (pI) of 8.04. Previous studies have shown that proteins with low MW (<110 kDa) are regarded as attractive vaccine targets, as they can be easily purified. In addition, transmembrane helix analysis revealed that DnaJ is a preferred target, as it has no transmembrane helix and can therefore be easily cloned and expressed.

Protein structure modelling and validation

The DnaJ protein three-dimensional (3D) structure was subjected to the PdbSum server to assess the Ramachandran plot statistics. The plot showed that 83.3% of the residues were present in the most favoured core regions (yellow colour), 12.2% in the additionally allowed region (yellow colour) and 0.8% in the generously allowed region (pale yellow colour) (Figure 1A). The results showed that the model structure had good quality and high stability and could be used for further study. The full DnaJ protein 3D structure model is shown in Figure 1B.

B-cell epitope prediction and evaluation

The B-cell linear epitope in DnaJ was predicted using Immune Epitope Database (IEDB) and the BepiPred 2.0. The results showed that BepiPred 2.0 predicted seven epitopes, whereas ABCpred predicted eight epitopes. ElliPro predicted six discontinuous B-cell epitopes in the DnaJ 3D structure (Figure 1C). Interestingly, all the predicted linear and structural B cell epitopes maintained their VaxiJen scores of >0.4.

T-cell epitope prediction and assessment

The human leukocyte antigen (HLA) class I-restricted T cell epitopes were predicted using the NetMHCpan 4.0 EL algorithm available at IEDB, using the method described by Paul et al [19]. Based on the final ranking scores (1% scoring peptides), we obtained eight cytotoxic T lymphocyte (CTL) epitopes. In parallel, following a previously reported approach [20], we used the Tepitool resource in IEDB and identified seven CTL epitopes in the DnaJ sequence.

rDnaJ expression and purification

rDnaJ was successfully expressed in *E. coli* following the induction with isopropyl-β-d-1-thiogalactopyranoside (IPTG) (0.5 mM). The sodium dodecyl sulphate polyacrylamide gel electrophoresis (SDS-PAGE) results revealed a protein of ~41.79 kDa MW (Figure 2B). rDnaJ was purified by nickel-nitrilotriacetic acid (Ni-NTA) affinity chromatography and the purity was more than 90% (Figure 2C). Subsequently, protein purification was confirmed by western blot analysis using Anti-His and Anti-*U. urealyticum*-infected mouse serum (Uu-serum) (as primary antibodies) (Figure 2D).

DnaJ immunisation induced DnaJ-specific antibody and cell-mediated immunity responses in mice

To determine the role of DnaJ in humoral immune response, DnaJ-specific antibody levels in the mouse serum were measured. Compared with those of the phosphate-buffered saline (PBS) and Freund's adjuvant (FA) groups, the DnaJ-immunised mice generated considerable immunoglobulin G (IgG) antibody titres over time (Figure 3A). To further characterise IgG isotype distribution (IgG1, IgG2a, IgG2b and IgG3) present in the serum, we performed an enzyme-linked immunosorbent assay (ELISA) to determine these antibody levels. A significant amount of serum IgG subclass antibodies was detected in the DnaJ-vaccinated mice. The serum IgG subclass antibody (IgG1, IgG2a and IgG3) levels induced in the recombinant antigen DnaJ group were also higher than those in the FA and PBS groups (Figure 3B). The responses were indicative of the Th1 response to IgG2a and IgG3 antibodies that were as easy to detect as IgG1 antibodies (Figure 3B). We also observed that DnaJ-immunised mouse serum but not control mouse serum recognised the purified DnaJ protein by western blot analysis (Figure 3C).

Previous studies have demonstrated that Th1 immune responses reduce the severity of cervicitis caused by *U. urealyticum*. To explore the type of cell-mediated immunity responses elicited by DnaJ immunisation, we first identified the cytokine levels in the splenocyte culture supernatants after stimulation during ELISA. Classical TNF-α and IFN-γ (Th1 cytokines) secretion was increased in DnaJ-immunised animals (Figure 4A), whereas IL-4 and IL-10 (Th2 cytokines) levels were nearly undetectable. We also observed a significant increase in the IFN-γ^+ $CD4^+$ T and IFN-γ^+ $CD8^+$ T cell percentages in DnaJ-immunised mouse splenocytes (Figure 4B). Conversely, we did not observe such a difference in the IL-

4^+ $CD4^+$ T cell percentage. These results suggested that DnaJ vaccination leads to a Th1 polarisation response.

DnaJ immunisation reduces the bacterial burden and inflammatory response in the cervix caused by U. urealyticum

The ability to confer protection against infection is a critical feature of a valid *U. urealyticum* vaccine. As described above, the mice were vaccinated with DnaJ and infected with *U. urealyticum* (1×10^7 colony-forming units (CFUs)/30 μL). On day 14 post-infection, we observed that all mice exhibited increased vaginal secretions, hair loss, vaginal redness and swelling, but the DnaJ-immunised group had relatively mild symptoms (Figure 5A). The bacterial burden in the cervix was determined by qPCR at 14 d post-challenge. As expected, immunisation with rDnaJ resulted in decreased *U. urealyticum* load in the primary lesion site (cervix) in the DnaJ-immunised mouse groups than in the control groups (Figure 5B, PBS or FA groups, $P < 0.05$).

To further understand how DnaJ immunisation mediates protection against *U. urealyticum*, we examined cytokine levels in the cervical tissue. IFN-γ, TNF-α, monocyte chemoattractant protein-1 (MCP-1) and IL-1β levels in the DnaJ-immunised mouse cervical tissue homogenate supernatants were reduced compared with those in the control supernatants (PBS or FA groups, $P < 0.05$, Figure 5C). Nevertheless, no difference in IL-1α, IL-17a, IL-6, and IL-10 levels was observed between the groups. Overall, DnaJ immunisation significantly lowered the cervix bacterial burden and inflammatory response during *U. urealyticum* challenge.

Protection against cervix pathological changes with DnaJ immunisation

U. urealyticum causes cervicitis associated with acute inflammation, oedema and cervical injury during infection. To further understand the protective effect of DnaJ, the mice were immunised, and at day 14 post-*U. urealyticum* infection, the cervix was compared for pathological changes in all groups of mice. The DnaJ-immunised mice had a lower inflammatory cell (such as polymorphonuclear leukocytes) recruitment than that of the control group (Figure 6A). Additionally, the cervical tissue sections from the PBS and FA groups showed severe pathological features such as epithelial shedding/necrosis within the uterine lumen, increased glandular secretions and dilated glandular ducts. Conversely, DnaJ-immunised mice showed cervical tissues with an intact endometrial layer with tubular structures and a clear small lumen.

We also assessed the cervical tissue after the challenge with *U. urealyticum* using immunohistochemistry. As shown in Figure 6B, the *U. urealyticum* antigen abundance (positive signal is a

brownish-yellow stain) was significantly reduced in the cervical glandular duct in DnaJ-immunised mice compared with those in the PBS- or FA-immunised mice. Overall, DnaJ immunisation was effective in reducing the infectious *U. urealyticum* load in the cervix.

DnaJ induces BMDC activation

DCs, professional antigen-presenting cells (APCs), are of particular interest during vaccination. To further determine whether *U. urealyticum* DnaJ induces DC activation, we first examined inflammatory cytokine secretion by DnaJ-stimulated BMDCs in cultured supernatants. DnaJ exhibited a dramatic increase in IL-1β, IL-6, IL-12p70 and TNF-α production in a dose-dependent manner (Figure 7A). Additionally, we analysed surface molecule expression in BMDCs. DnaJ significantly increased surface molecule (CD80 and CD86) and MHC class II expression in BMDCs (Figure 7B). Therefore, DnaJ directly induced BMDC activation and maturation. Next, to investigate the possible contributions of trace amounts of residual lipopolysaccharide, DnaJ was subjected to polymyxin B (PMB) treatment and then inactivated by heat. PMB pre-treatment did not affect the DnaJ ability to trigger BMDC activation. However, heat inactivation significantly inhibited DnaJ (Figure 7B, compared with untreated DnaJ, $P<0.05$). Additionally, we found no remarkable differences in the cytosolic marker lactate dehydrogenase (LDH) release upon DnaJ stimulation (Supplementary Figure 2). In summary, DnaJ induced BMDC maturation independent of cell damage or contaminating endotoxins.

DnaJ-pulsed BMDCs promote CD4 Th1 immune responses

T helper 1 cell cytokines, especially IFN-γ, are critical for *U. urealyticum* clearance. To examine whether DnaJ-pulsed BMDCs induced the CD4 naïve T cells towards an IFN-γ-producing Th1 cell phenotype, ELISA was performed to examine Th1/Th2 cytokine expression in the BMDC-naïve T cell co-culture system. DnaJ-pulsed BMDCs significantly increased IFN-γ secretion by T cells (Figure 8A, compared with the DnaJ-BMDCs or BMDCs-T cell groups, $P<0.01$). In contrast, IL-4, IL-5 and IL-10 were not induced.

Finally, we vaccinated naïve mice with DnaJ-pulsed BMDCs, PBS-pulsed BMDCs or PBS (intravenous injection). As expected, the DnaJ-specific Th1 cells ($CD4^+IFN\text{-}\gamma^+$) were detected in the adoptive immunisation of mice with DnaJ-pulsed BMDCs (Figure 8B). However, we did not observe a significant difference in the percentage of Th2 cells ($CD4^+IL\text{-}4^+$) in the splenocytes of DnaJ-pulsed BMDC groups compared with that of the PBS-pulsed BMDCs or PBS groups. Next, we assessed the serum anti-DnaJ IgG1, IgG2a, IgG2b and IgG3 antibodies by ELISA and found that mice immunised with DnaJ-pulsed BMDCs showed a Th1-biased IgG2 antibody response (Figure 8C). Together, these results established that the use of DnaJ-pulsed BMDCs in vitro induces a Th1 immune response in vivo.

Discussion

Currently, no licenced vaccines against *U. urealyticum* are available [1,18]. Here, we showed that rDnaJ vaccination provided protection against *U. urealyticum* challenge. We also attempted to illustrate the increase in the robust Th1 immune reaction of Uu-DnaJ by showing that DnaJ interacts with DCs and improves vaccine development.

An effective vaccine immunogen should meet the following requirements: (1) it should be highly conserved among *U. urealyticum* serovars, (2) it should be expressed and antigenic during infection and (3) it should elicit long-term protective immunity in vivo [23,24]. We observed that *U. urealyticum*-infected mouse serum recognised rDnaJ. Thus, DnaJ was up-regulated during *U. urealyticum* infection suggesting that it is a potential antigen target [18,21]. The protein was expressed in *E. coli* BL21 (DE3). However, other biological impurities from the rDnaJ challenge may be used to develop safe vaccines [25,26]. In our study, rDnaJ was purified using Ni-affinity chromatography, and the DnaJ-immunised mouse serum did not recognise bacterial lysates converted to empty pET28a plasmids (see Figure 3C). Therefore, rDnaJ of *U. urealyticum*-induced immune response can be attributed to itself.

Some scholars have pointed out that recombinant protein subunit vaccines have limited intrinsic adjuvanticity and require immunogen formulation with adjuvants [27–29]. Previous reports indicated a key role of Th1 cells and neutralising antibodies in protection against pathogen challenge [30–32]. Therefore, we used a vaccine formulated with DnaJ and Th1 adjuvants (Freund's adjuvant) to elicit protection against genital *U. urealyticum* infection in mice. As expected, the humoral immune responses increased over time in the DnaJ-immunised group and induced strong antigen-specific cellular immunity responses (TNF-α and IFN-γ secretion dominant). Importantly, the DnaJ-specific immune response demonstrated effective protection—mice immunised with DnaJ (adjuvanted by Freund's adjuvant) and challenged 14 days after boosting exhibited a reduction in *U. urealyticum* load. Furthermore, the Th1 vaccination protocol has a pronounced effect on controlling the extent of inflammation and protects infected mice against cervical tissue pathology. Colonisation by *U. urealyticum* is related to increased levels of certain pro-inflammatory or inflammatory factors in the uterine cervix [18, 33, 34]. We observed that many TNF-α and IFN-γ-producing cells appeared in mice after immunisation with DnaJ. Despite this, low levels of inflammatory factors (including TNF-α and IFN-γ) were detected in the cervix tissue upon *U. urealyticum* infection. This may imply that the hallmark Th1 cytokines (IFN-γ and TNF-α) activate innate immune cells such as macrophages and DCs in the cervix for pathogen clearance [35–37]. Naturally, Th1 cytokine-activated DCs are also required for the optimal initiation of the host protective Th1 response [38]. However, our study has limitations, such as the interaction between innate and adaptive immune cells remaining poorly understood at the site of *U. urealyticum* infection (after DnaJ-vaccination). Future studies monitoring the recruitment of host immune cells in the cervix during *U. urealyticum* infection could help resolve this issue [25, 30].

Compared with macrophages, DCs are professional APCs with the ability to bridge innate and adaptive immunity and are necessary for optimal T-cell activation and differentiation [39]. Upon sensing inflammatory or infectious stimuli, DCs mature by upregulating co-stimulatory molecules and migrating to the draining lymph node to drive the T-cell response [40]. Our analyses of the collected supernatant

from the BMDCs activated by DnaJ indicated that the pro-inflammatory cytokine IL-12p70 levels exhibited a dose-dependent increase. Previous studies on DC-mediated IL-12p70 production were critical for initiating an optimal acquired-IFN-γ response from T cells [39, 41, 42]. In BMDC maturation, in addition to the production of cytokines, DnaJ induces BMDC activation, for example, CD80, CD86 and MHC class II upregulation. Thus, BMDC maturation by DnaJ treatment may be a key event that induces T-cell responses. This assertion was supported by in vitro studies using BMDC-T cell co-culture. In the co-culture system medium, IFN-γ levels remarkably increased compared with those of the control groups, which showed that DnaJ-stimulated BMDCs potently triggered naïve T cell polarisation towards a Th1 subset. Overall, *U. urealyticum* DnaJ increases BMDC maturation in a dose-dependent manner and drives the Th1 immune response [43].

DCs are crucial for the activation of the host immune system. We have shown that the effect of DnaJ on DCs skews naïve CD4 T cells to Th1-cell differentiation. Interestingly, Shaw et al. [44] indicated that the phenotype and function of ex vivo mature BMDCs may not necessarily predict the immune reactions established in vivo following adoptively transferred cells. In their study, they found that in BMDCs pulsed with *Chlamydia* spp, major outer membrane protein (MOMP) induced CD4 T cells to secrete IFN-γ ex vivo. However, MOMP-pulsed BMDC adoptive immunisation induced a Th2- rather than a Th1-polarised immune response. To investigate the role of mature BMDCs with DnaJ in Th1 or Th2 polarisation in vivo, mice were immunised with DnaJ-pulsed DCs. We found that Th1 cells were more abundant in the DnaJ-pulsed BMDCs group, whereas no changes in the percentage of Th2 cells in the control groups were observed, which clearly depicted the pro-host immunological properties of this protein antigen. Unlike the mice immunised with DnaJ and Freud's adjuvant, autologous DCs loaded with DnaJ induced a Th1 immune response without bias. We refrained from using an exogenous adjuvant because of its inherent ability to skew the immunological response to vaccine antigens, such as Th1 or Th2 responses [45,46]. Safe and non-toxic adjuvants (including DCs) could induce stronger and more efficacious immune responses when compared to recombinant proteins alone [47,48]. However, many challenges in adoptive DC immunotherapy, such as cost, tedious operation and enough quantity of functional autologous DCs that cannot always be obtained still exist, therefore, finding a desirable adjuvant to synergistically enhance a DnaJ-induced Th1 response rather than a Th2 response, which could provide a promising strategy for developing a safe, inexpensive and effective *U. urealyticum* vaccine, is necessary [49].

Conclusion

In summary, immunisation with Uu-DnaJ could induce both antigen-specific antibodies and cellular immune responses and promote sterilising immunity. Furthermore, Uu-DnaJ could promote the maturation of DCs, which leads to a Th1 immune response in the host. The isolation and characterisation of heat-shock stress-response antigens of *U. urealyticum* will not only help in the rational design of efficacious vaccines but also aid immunopathogenesis studies of *U. urealyticum* infection.

Declarations

Authors' contributions

FYG, YHT, WJZ, HXY, JX, WYT, RHL and GZD, contributed to the study design and data interpretation. All authors reviewed, provided critical feedback and helped in shaping the final version of the manuscript. All authors approved the final draft of the manuscript and are accountable for the accuracy and integrity of the work. All authors read and approved the final manuscript.

Availability of data and material

The datasets generated and analyzed in the current study are available from the corresponding author upon reasonable request.

Funding

This work was chiefly supported by funds from the Hunan Provincial Innovation Foundation For Postgraduate (NO. CX20200982), the Research Project of Hunan Provincial Health and Wellness Commission (NO. B2019003), the Hunan Science and Technology Innovation Project (NO. 2018SK50302), the Hunan Provincial Department of Education Project (NO. 19B496) and the Natural Science Foundation of Hunan Province (NO. 2020JJ4521)

Ethics approval and consent to participate

All animal-related protocols were approved by the Institutional Animal Use Committee of the University of South China.

Consent for publication

Not applicable

Competing interests

No potential conflict of interest was reported by the author(s).

References

1. Sweeney EL, Dando SJ, Kallapur SG, et al. The Human Ureaplasma Species as Causative Agents of Chorioamnionitis. Clin Microbiol Rev. 2016,30(1):349-379.
2. Glass JI, Lefkowitz EJ, Glass JS, et al. The complete sequence of the mucosal pathogen Ureaplasma urealyticum. Nature. 2000,407(6805):757-62.
3. Taylor-Robinson D. Mollicutes in vaginal microbiology: Mycoplasma hominis, Ureaplasma urealyticum, Ureaplasma parvum and Mycoplasma genitalium. Res Microbiol. 2017,168(9-10):875-881.

4. Zanotta N, Campisciano G, Morassut S, et al. Emerging role for Ureaplasma parvum serovar 3: Active infection in women with silent high-risk human papillomavirus and in women with idiopathic infertility. J Cell Physiol. 2019,234(10):17905-17911.
5. Triantafilou M, De Glanville B, Aboklaish AF, et al. Synergic activation of toll-like receptor (TLR) 2/6 and 9 in response to Ureaplasma parvum & urealyticum in human amniotic epithelial cells. PLoS One. 2013,8(4):e61199.
6. Sprong KE, Mabenge M, Wright CA, Govender S. Ureaplasma species and preterm birth: current perspectives. Crit Rev Microbiol. 2020,46(2):169-181.
7. Waites KB, Crabb DM, Xiao L, et al. In Vitro Activities of Eravacycline and Other Antimicrobial Agents against Human Mycoplasmas and Ureaplasmas. Antimicrob Agents Chemother. 2020, 64(8):e00698-20.
8. Bebear CM, Renaudin H, Charron A,et al. In vitro activity of trovafloxacin compared to those of five antimicrobials against mycoplasmas including Mycoplasma hominis and Ureaplasma urealyticum fluoroquinolone-resistant isolates that have been genetically characterized. Antimicrob Agents Chemother. 2000,44(9):2557-60.
9. Yang T, Pan L, Wu N, et al. Antimicrobial Resistance in Clinical Ureaplasma spp. and Mycoplasma hominis and Structural Mechanisms Underlying Quinolone Resistance. Antimicrob Agents Chemother. 2020,64(6):e02560-19.
10. Abbas G, Zafar I, Ahmad S, et al. Immunoinformatics design of a novel multi-epitope peptide vaccine to combat multi-drug resistant infections caused by Vibrio vulnificus. Eur J Pharm Sci. 2020 ,142:105160.
11. Dai G, Li R, Chen H, et al. A ferritin-like protein with antioxidant activity in Ureaplasma urealyticum. BMC Microbiol. 2015,15:145.
12. Qin L, Chen Y, You X. Subversion of the Immune Response by Human Pathogenic Mycoplasmas. Front Microbiol. 2019,10:1934.
13. Zügel U, Kaufmann SH. Immune response against heat shock proteins in infectious diseases. Immunobiology. 1999, 201(1):22-35.
14. Colaco CA, Bailey CR, Walker KB, et al. Heat shock proteins: stimulators of innate and acquired immunity. Biomed Res Int. 2013,2013:461230.
15. Matsui HM, Hazama S, Nakajima M, et al. Novel adjuvant dendritic cell therapy with transfection of heat-shock protein 70 messenger RNA for patients with hepatocellular carcinoma: a phase I/II prospective randomized controlled clinical trial. Cancer Immunol Immunother. 2021,70(4):945-957.
16. Fang L, Sun L, Yang J, et al. Heat shock protein 70 from Trichinella spiralis induces protective immunity in BALB/c mice by activating dendritic cells. Vaccine. 2014,32(35):4412-4419.
17. Bracher A, Verghese J. GrpE, Hsp110/Grp170, HspBP1/Sil1 and BAG domain proteins: nucleotide exchange factors for Hsp70 molecular chaperones. Subcell Biochem. 2015,78:1-33.
18. Tang Y, Guo F, Lei A, et al. GrpE Immunization Protects Against Ureaplasma urealyticum Infection in BALB/C Mice. Front Immunol. 2020,11:1495.

19. Paul S, Lindestam Arlehamn CS, Scriba TJ, et al. Development and validation of a broad scheme for prediction of HLA class II restricted T cell epitopes. J Immunol Methods. 2015,422:28-34.
20. Grifoni A, Sidney J, Zhang Y, et al. A Sequence Homology and Bioinformatic Approach Can Predict Candidate Targets for Immune Responses to SARS-CoV-2. Cell Host Microbe. 2020,27(4):671-680.e2.
21. Kim WS, Jung ID, Kim JS, et al. Mycobacterium tuberculosis GrpE, A Heat-Shock Stress Responsive Chaperone, Promotes Th1-Biased T Cell Immune Response via TLR4-Mediated Activation of Dendritic Cells. Front Cell Infect Microbiol. 2018,8:95.
22. Inaba K, Inaba M, Romani N, Aya H, Deguchi M, Ikehara S, Muramatsu S, Steinman RM. Generation of large numbers of dendritic cells from mouse bone marrow cultures supplemented with granulocyte/macrophage colony-stimulating factor. J Exp Med. 1992,176(6):1693-702.
23. Li P, Liu Q, Luo H, et al. Bi-valent polysaccharides of Vi capsular and O9 O-antigen in attenuated Salmonella Typhimurium induce strong immune responses against these two antigens. NPJ Vaccines. 2018,3:1.
24. Eslamizar L, Petrovas C, Leggat DJ, et al. Recombinant MVA-prime elicits neutralizing antibody responses by inducing antigen-specific B cells in the germinal center. NPJ Vaccines. 2021,6(1):15.
25. Sen-Kilic E, Blackwood CB, Boehm DT, et al. Intranasal Peptide-Based FpvA-KLH Conjugate Vaccine Protects Mice From Pseudomonas aeruginosa Acute Murine Pneumonia. Front Immunol. 2019,10:2497.
26. Akache B, Agbayani G, Stark FC, et al. Sulfated Lactosyl Archaeol Archaeosomes Synergize with Poly(I:C) to Enhance the Immunogenicity and Efficacy of a Synthetic Long Peptide-Based Vaccine in a Melanoma Tumor Model. Pharmaceutics. 2021,13(2):257.
27. Pal S, Cruz-Fisher MI, Cheng C, Carmichael JR, et al. Vaccination with the recombinant major outer membrane protein elicits long-term protection in mice against vaginal shedding and infertility following a Chlamydia muridarum genital challenge. NPJ Vaccines. 2020 ,5(1):90.
28. Brunham RC, Rappuoli R. Chlamydia trachomatis control requires a vaccine. Vaccine. 2013 Apr 8,31(15):1892-7.
29. Farris CM, Morrison SG, Morrison RP. CD4+ T cells and antibody are required for optimal major outer membrane protein vaccine-induced immunity to Chlamydia muridarum genital infection. Infect Immun. 2010,78(10):4374-83.
30. Zhao J, Zhao J, Mangalam AK, et al. Airway Memory CD4(+) T Cells Mediate Protective Immunity against Emerging Respiratory Coronaviruses. Immunity.
31. Ye L, Jiang Y, Yang G, et al. Murine bone marrow-derived DCs activated by porcine rotavirus stimulate the Th1 subtype response in vitro. Microb Pathog. 2017,110:325-334.
32. Li Y, Zheng K, Tan Y, et al. A recombinant multi-epitope peptide vaccine based on MOMP and CPSIT_p6 protein protects against Chlamydia psittaci lung infection. Appl Microbiol Biotechnol. 2019,103(2):941-952.
33. Viscardi RM, Kaplan J, Lovchik JC, et al. Characterization of a murine model of Ureaplasma urealyticum pneumonia. Infect Immun. 2002,70(10):5721-9.

34. von Chamier M, Allam A, Brown MB, et al. Host genetic background impacts disease outcome during intrauterine infection with Ureaplasma parvum. PLoS One. 2012,7(8):e44047.
35. Back YW, Bae HS, Choi HG, et al. Fusion of Dendritic Cells Activating Rv2299c Protein Enhances the Protective Immunity of Ag85B-ESAT6 Vaccine Candidate against Tuberculosis. Pathogens. 2020 Oct 22,9(11):865.
36. Noya V, Brossard N, Rodríguez E, et al. A mucin-like peptide from Fasciola hepatica instructs dendritic cells with parasite specific Th1-polarizing activity. Sci Rep. 2017 ,7:40615.
37. ollyky PL, Evanko SP, Wu RP, et al. Th1 cytokines promote T-cell binding to antigen-presenting cells via enhanced hyaluronan production and accumulation at the immune synapse. Cell Mol Immunol. 2010,7(3):211-20.
38. Gold MC, Ehlinger HD, Cook MS, et al. Human innate Mycobacterium tuberculosis-reactive alphabetaTCR+ thymocytes. PLoS Pathog. 2008 ,4(2):e39.
39. Thomas R, Wang S, Shekhar S, et al. Semaphorin 3E Protects against Chlamydial Infection by Modulating Dendritic Cell Functions. J Immunol. 2021,206(6):1251-1265.
40. Choi S, Choi HG, Lee J, et al. Mycobacterium tuberculosis protein Rv2220 induces maturation and activation of dendritic cells. Cell Immunol. 2018 ,328:70-78.
41. Varikuti S, Verma C, Natarajan G, et al. MicroRNA155 Plays a Critical Role in the Pathogenesis of Cutaneous Leishmania major Infection by Promoting a Th2 Response and Attenuating Dendritic Cell Activity. Am J Pathol. 2021,191(5):809-816.
42. Barhoumi M, Koutsoni OS, Dotsika E, et al. Leishmania infantum LelF and its recombinant polypeptides induce the maturation of dendritic cells in vitro: An insight for dendritic cells based vaccine. Immunol Lett. 2019,210:20-28.
43. Lü H, Wang H, Zhao HM, et al. Dendritic cells (DCs) transfected with a recombinant adenovirus carrying chlamydial major outer membrane protein antigen elicit protective immune responses against genital tract challenge infection. Biochem Cell Biol. 2010,88(4):757-65.
44. Shaw J, Grund V, Durling L, et al. Dendritic cells pulsed with a recombinant chlamydial major outer membrane protein antigen elicit a CD4(+) type 2 rather than type 1 immune response that is not protective. Infect Immun. 2002,70(3):1097-105.
45. Arora SK, Alam A, Naqvi N, et al. Immunodominant Mycobacterium tuberculosis Protein Rv1507A Elicits Th1 Response and Modulates Host Macrophage Effector Functions. Front Immunol. 2020,11:1199.
46. Agger EM, Cassidy JP, Brady J, et al. Adjuvant modulation of the cytokine balance in Mycobacterium tuberculosis subunit vaccines, immunity, pathology and protection. Immunology. 2008,124(2):175-85.
47. Lindblad EB, Elhay MJ, Silva R, et al. Adjuvant modulation of immune responses to tuberculosis subunit vaccines. Infect Immun. 1997,65(2):623-9.
48. Ciabattini A, Pettini E, Fiorino F, et al. Modulation of Primary Immune Response by Different Vaccine Adjuvants. Front Immunol. 2016,7:427.

49. Knudsen NP, Olsen A, Buonsanti C, et al. Different human vaccine adjuvants promote distinct antigen-independent immunological signatures tailored to different pathogens. Sci Rep. 2016,6:19570.

Figures

Figure 1

Bioinformatics analysis of DnaJ based on the amino acid sequences. (A) Ramachandran plots, (B) three-dimensional (3D) structure of DnaJ, (C) Conformational B-cell epitopes of DnaJ.

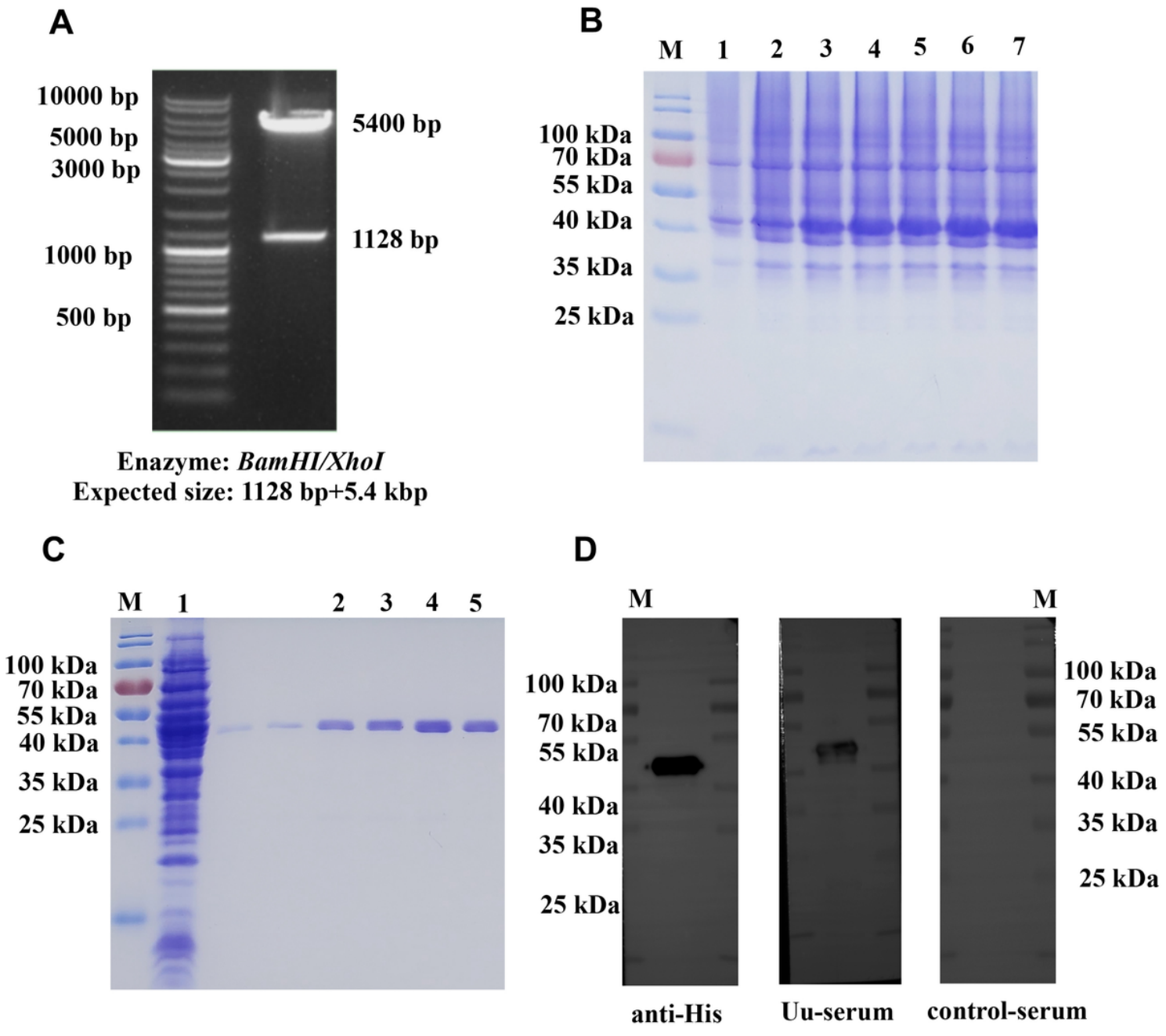

Figure 2

Enzyme digestion results. (A) Polymerase chain reaction successfully amplified the expected DnaJ gene band (1128 bp) and the DnaJ gene in Escherichia coli BL21 was cloned using the pET-28a vector and BamI and XhoI restriction sites. Preparation of the recombinant DnaJ protein: (B) DnaJ was over-expressed in E. coli BL21 (lanes 3–7), (C) 12.5% sodium dodecyl sulphate -polyacrylamide gel electrophoresis analysis of the DnaJ protein purification (lanes 1, uninduced, lanes 2–5, DnaJ was purified by using eluates of 100, 150, 200 and 250 mM of imidazole), (D) Western blot analysis of the DnaJ protein using anti-His, Uu-serum and control serum.

Figure 3

Detection of the DnaJ-specific antibodies in immunised mice. (A) Anti-DnaJ Ig G antibody titres (n = 4 mice per group), (B) Elicited IgG subclass (IgG1, IgG2b and IgG2a) in vaccinated mice (n = 4 mice per group). (C) Western blot analysis of purified DnaJ (C, Lane 2, 4, 6 and 8) and the lysate of bacteria transformed with the empty pET28a plasmid (C, Lane 1, 3, 5 and 7) using mouse anti-His antibodies, DnaJ-immunised mouse serum, phosphate-buffered saline- and Freund's adjuvant-mouse serum.

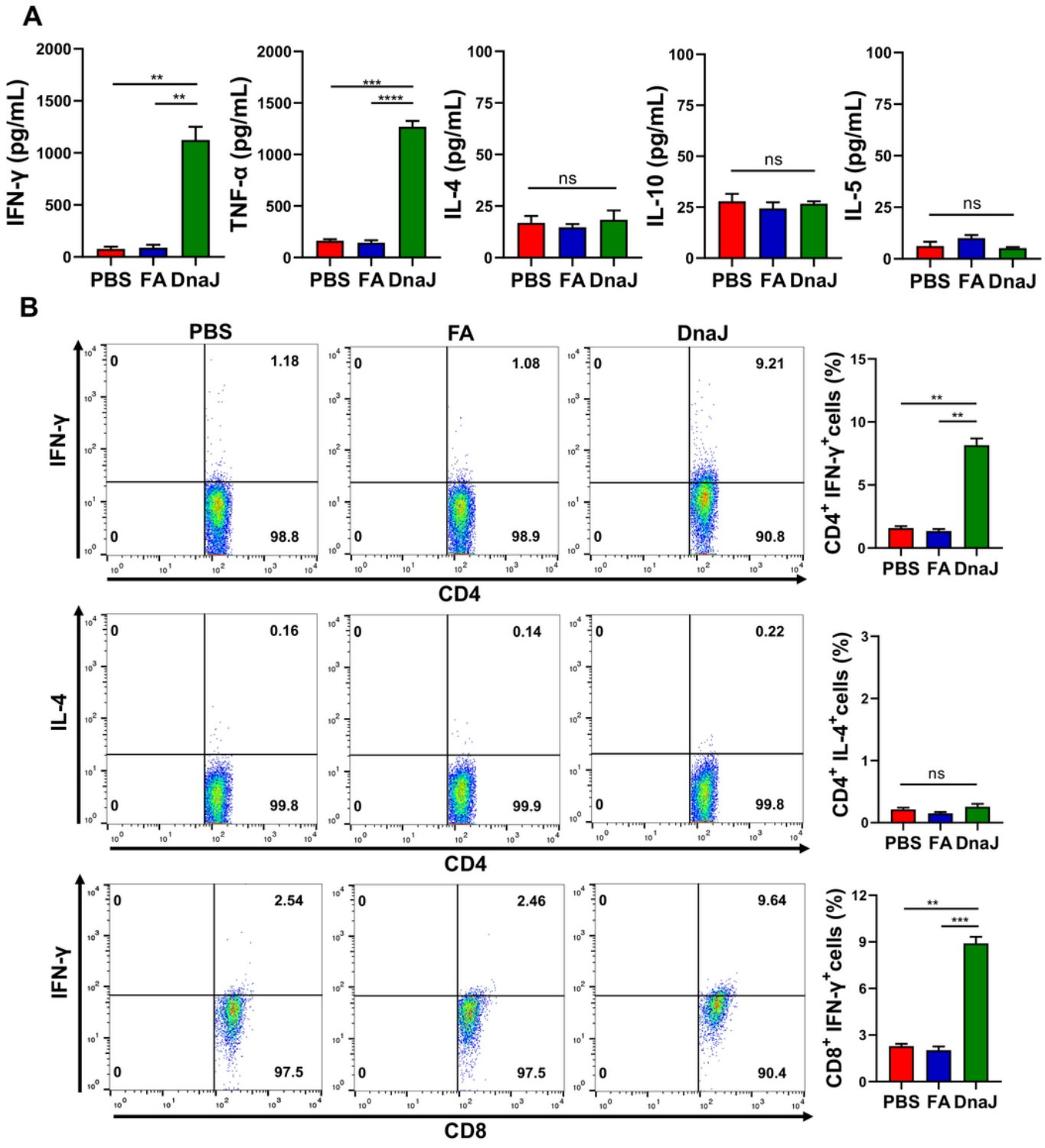

Figure 4

The DnaJ vaccine with FA predominantly induces Th1-cytokine production in mice. (A) The splenocytes were isolated from phosphate-buffered saline-, FA-, and DnaJ-vaccinated groups and stimulated with 10 μg of DnaJ for 48 h in vitro. The levels of IFN-γ, TNF-α, IL-4, and IL-10 in the cell supernatants were measured by enzyme-linked immunosorbent assay (n = 4 mice per group). **P <0.01, ***P <0.001, ****P <0.0001, and ns = not significant, P >0.05. (B) The DnaJ vaccine with FA induced the generation of IFN-γ-

secreting CD4+ and CD8+cells: Proportion of IFN-γ+ CD4+cells in the splenocytes. The proportion of IL-4+ CD4+cells in the splenocytes. The proportion of IFN-γ+ CD8+cells in the splenocytes. **P <0.01, ***P <0.001, and ns = not significant, P >0.05.

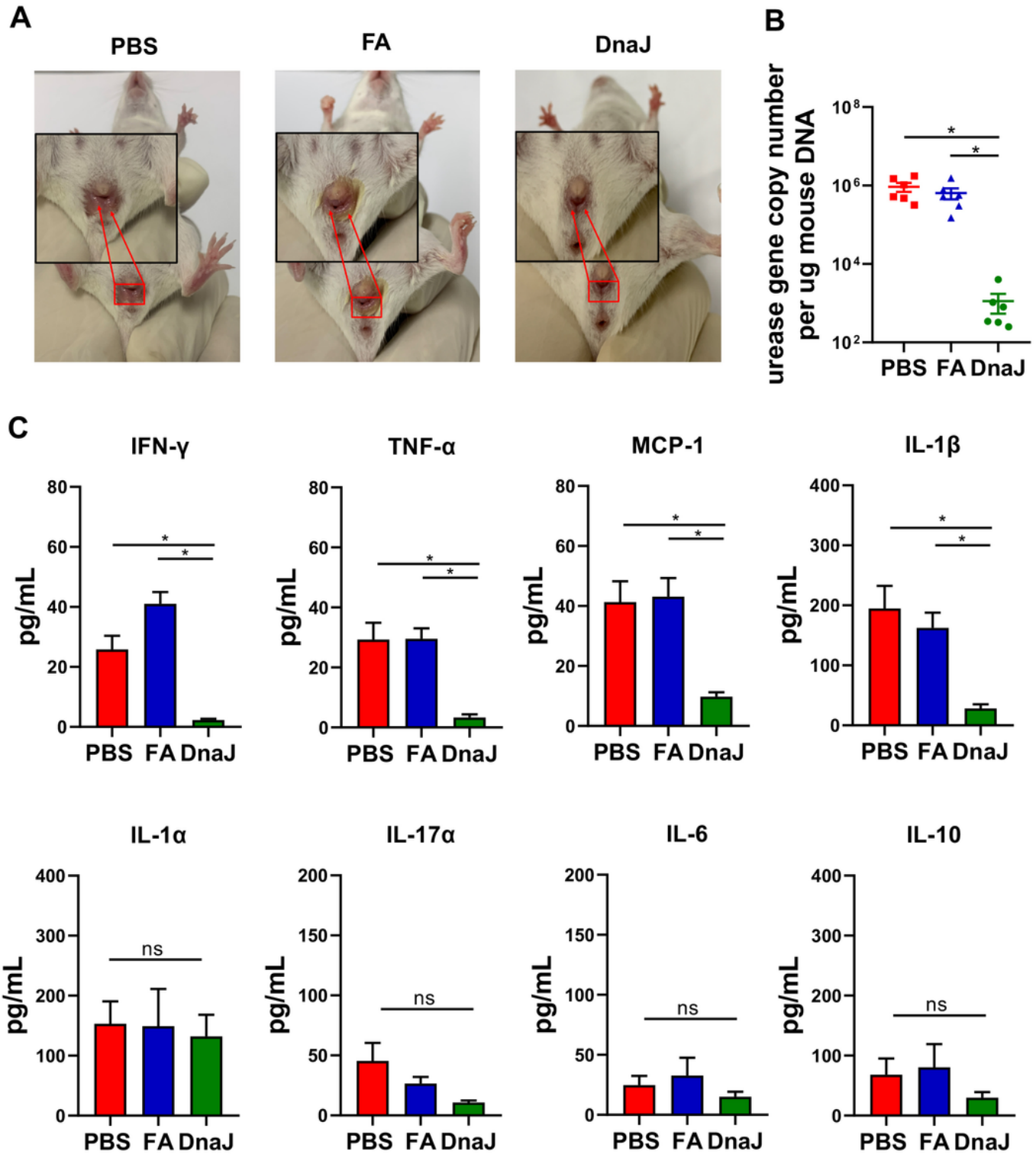

Figure 5

DnaJ-immunisation reduced Ureaplasma urealyticum load and inflammatory response in the reproductive tract of infected mice: (A) Representative photographs of the vulva in mice 14 days after

infection. (B) The burden of U. urealyticum in diseased cervical tissue was measured by quantitative polymerase chain reaction of the urease gene concentration (n = 6 mice per group). *P <0.05. (C) Cytokine concentrations in the cervical tissue of U. urealyticum-infected mice. Concentrations of IL-1α, TNF-α, IFN-γ, MCP-1, IL-1β, IL-10, IL-17a and IL-6 in the supernatant of the cervical tissue homogenates from the mice after U. urealyticum infection, as determined using a multi-analyte flow assay kit. The cytokine concentrations (pg/mL) in the cervical tissue homogenate (n = 3–6 mice per group). *P <0.05, and ns = not significant, P >0.05.

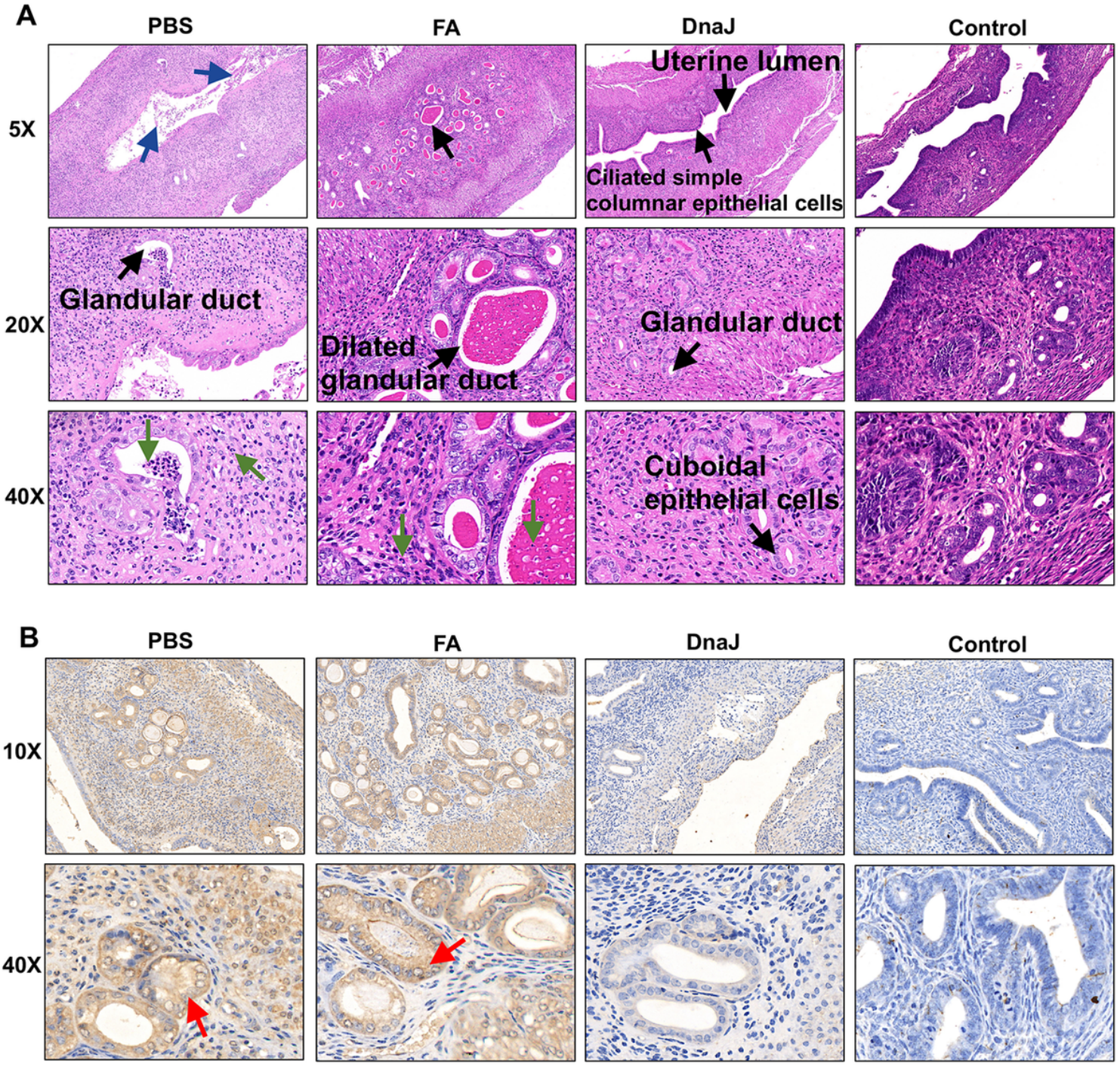

Figure 6

Pathological lesions of the infected cervical tissues: (A) Haematoxylin and eosin staining in the cervical tissue of each group. The black arrows denote uterine lumen, endometrial layer or glandular duct. The blue arrows denote regions of epithelial shedding/necrosis within the uterine lumen. The green arrows indicate inflammatory cells or necrotic cell debris. (B) Evaluation of Ureaplasma urealyticum load in the infected cervical tissue using immunohistochemistry. The cervical tissue was removed from phosphate-buffered saline-, Freund's adjuvant-, and DnaJ-injected mice (14 days after challenge with U. urealyticum). Naïve mice were included as a negative control group (uninfected with U. urealyticum). Sections were stained with a mouse anti-U. urealyticum. The red arrows indicate the cervical tissue cells that contain U. urealyticum (areas stained brown).

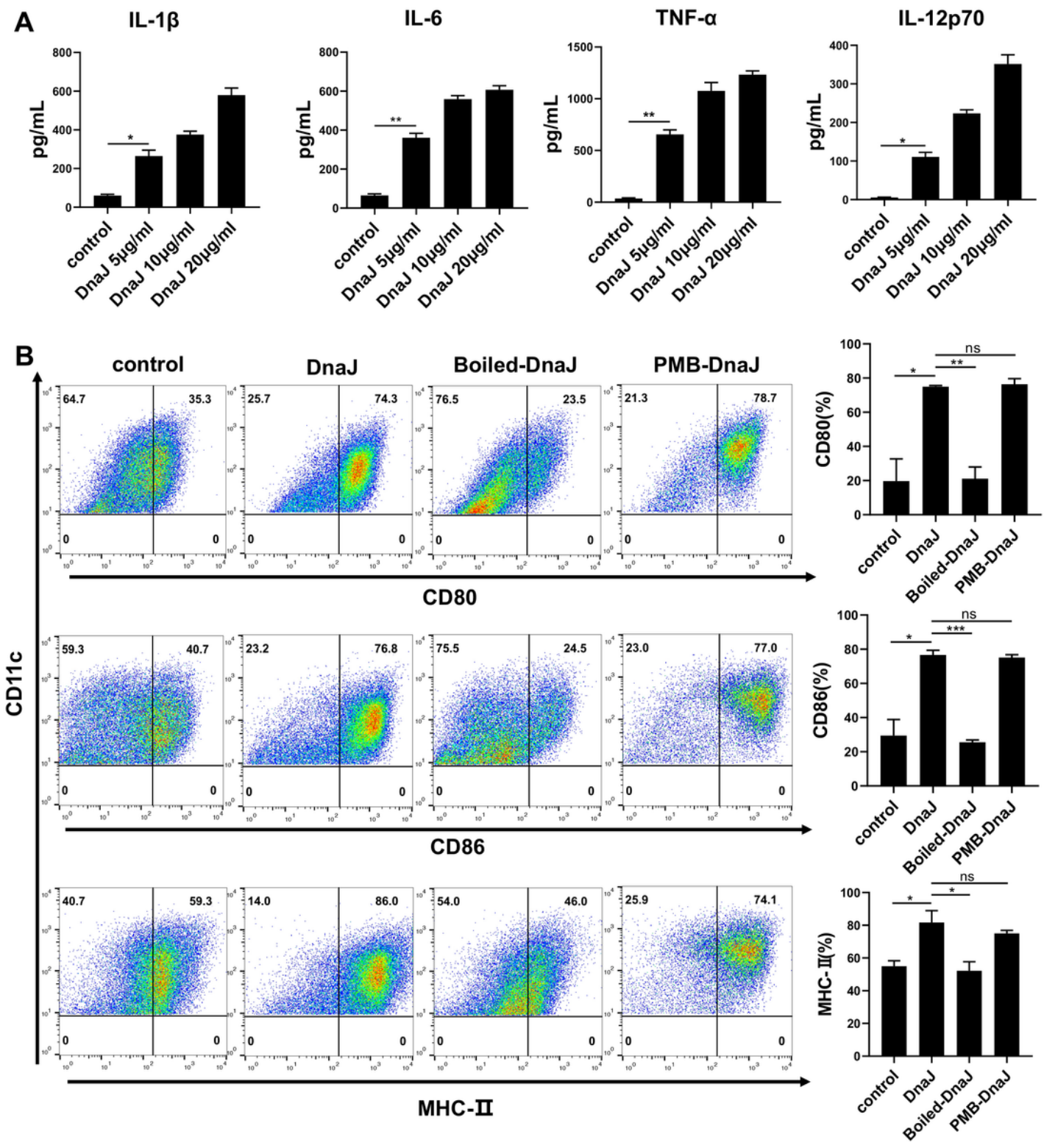

Figure 7

DnaJ induces BMDC activation: (A) Immature BMDCs were stimulated with 5–20 μg/mL DnaJ for 24 h. Analysis of IL-1β, IL-6, IL-12p70 and TNF-α production through enzyme-linked immunosorbent assay, *P <0.05 and **P <0.01. Immature BMDCs were treated with 10 μg/mL DnaJ. Alternatively, DCs were stimulated with DnaJ digested with polymyxin B for 3 h at 4 °C or heated at 100 °C for 2 h. After 24 h, the expression of surface molecules in the cluster of CD11c+ BMDCs were measured. (B) Representative

plots of CD80, CD86 and MHC-II on BMDCs detected from three independent experiments are shown (C) Analysis of expression percentages of the surface molecules on BMDCs, *P <0.05, **P <0.01 and ns = not significant, P >0.05. The data are representative of three independent experiments.

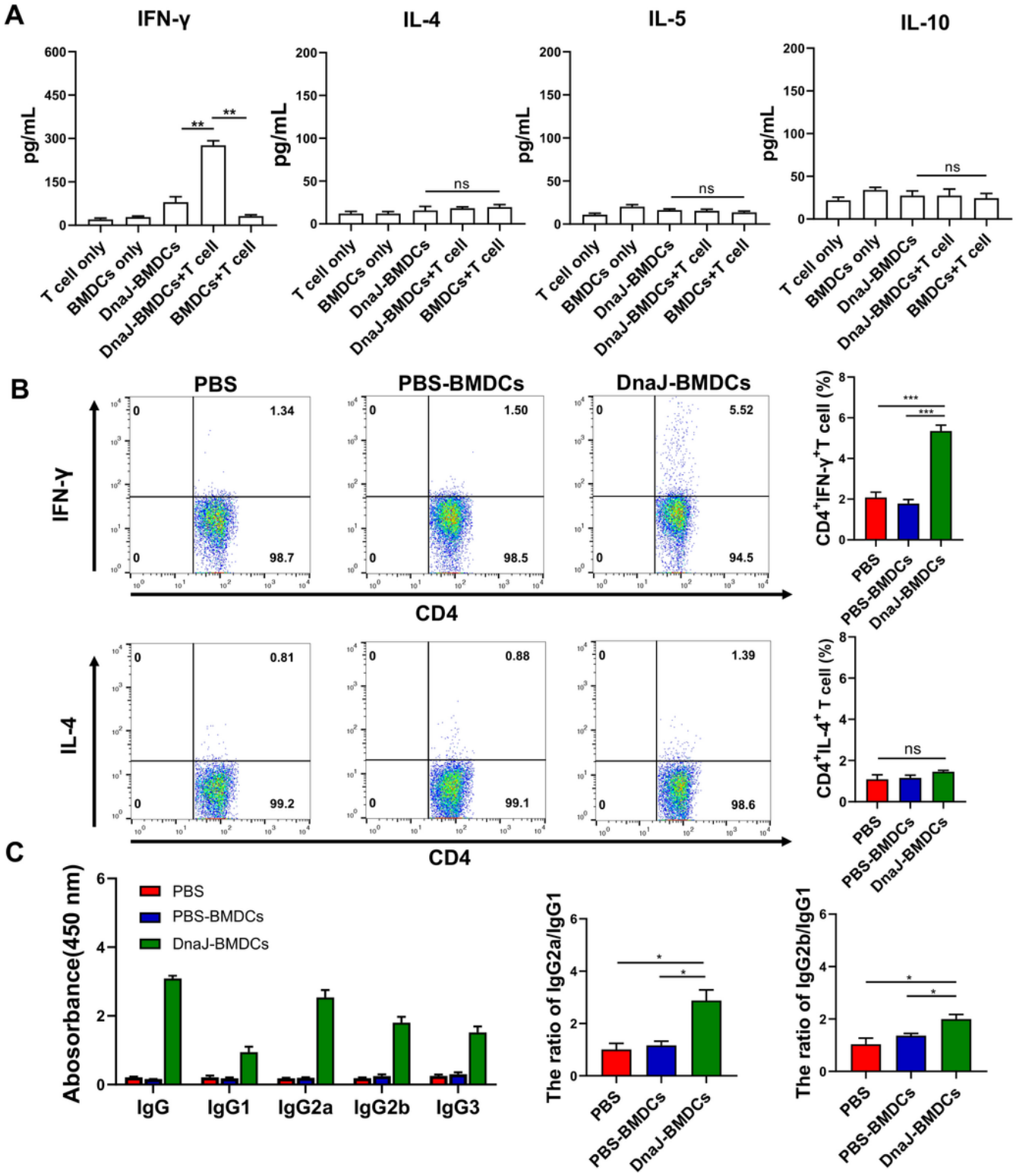

Figure 8

Regulation of Th1 polarisation by DnaJ via BMDC modulation: (A) Polarisation of the cluster of differentiation CD4 naïve T cells by DnaJ-treated BMDCs. At 3 days after co-culture, IFN-γ, iIL-4, IL-5 and

IL-10 levels in the co-culture supernatants were analysed by ELISA, **P <0.01 and ns = not significant, P >0.05. The data are representative of three independent experiments. Immune responses after adoptive immunisation of DnaJ-pulsed BMDCs: (B) The splenocytes from the mice of each group were cultured in DnaJ for 8 h (n = 4 mice per group). A flow cytometry assayed the proportion of the activated T helper (Th)1 cells and Th2 cells in the splenocytes. ***P <0.001 and ns = not significant, P >0.05. (C) ELISA of DnaJ-specific IgG subtypes (IgG1, IgG2b, IgG2a and IgG3) levels in the adoptive immune sera and the calculated IgG2a/IgG1 and IgG2b/IgG1 ratio. *P <0.05.

Supplementary Files

This is a list of supplementary files associated with this preprint. Click to download.

- FigureS1.docx
- FigureS2.docx